BMC Genomics

RESEARCH Open Access

Genome-wide analysis of fatty acid desaturase genes in moso bamboo (*Phyllostachys edulis*) reveal their important roles in abiotic stresses responses

Chun Fu[1], Qinchao Fu[1], Shanshan Wang[2], Fangzhou Wu[2], Na Jiang[3], Ruoqi Zhou[2], Yaojun Yang[1] and Yufei Xue[2*]

Abstract

Background Bamboo is an important nontimber forestry product worldwide, while growth, development and geographic distribution of bamboo are often affected by abiotic stresses. Fatty acid desaturases have important roles in regulating plant abiotic stress tolerance, especially low-temperature. However, there is no report on genome-wide of *FAD* genes in bamboo under abiotic stresses.

Results A toltal of 43 *PeFAD* genes were identified in moso bamboo genome, which were unevenly located in 17 scaffolds. Phylogenetic analysis indicated that *PeFAD* genes were divided into 6 groups and ADS/FAD5 group was absence in momo bamboo, and gene structure and histidine-motifs remained highly conserved in each group. The expansion of *PeFAD* genes was mainly caused by tandem and segmental duplications of *SAD/FAB2* group. We also identified 59 types of miRNAs targeting *PeFAD* genes. RNA-seq data indicated that *PeFAD* genes were transcribed in various organs/tissues with different degrees, and responded to abiotic stresses and hormone treatments, including cold, salt, drought, SA, ABA, BR, NAA and GA. Co-expression analysis under cold stress showed that PeCBF3 might directly bind the promoter of top cold-responsive *PeSLD1* gene that contained LTR *cis*-element and DRE core element. The qRT-PCR assay also validated the expression pattern of *PeSLD1* and its upstream regulatory gene *PeCBF3*.

Conclusion In this study, we performed comprehensive genome-wide survey of *PeFAD* genes in moso bamboo and analyzed their expression patterns in various tissues and organs, and under abiotic stresses and phytohormones treatment. The qRT-PCR assay validated the cold inducibility of *PeSLD1* and *PeCBF3*. This work showed critical roles of *PeFAD* genes in abiotic stresses responses. This is the first report on genome-wide analysis of *PeFAD* genes in moso bamboo, which will provide critical gene resources for molecular breeding of stress-toleranct moso bamboo.

Keywords Moso bamboo (*Phyllostachys edulis*), Fatty acid desaturase, Genome-wide identification, Phylogenetic analysis, Expression analysis, Abiotic stresses

*Correspondence:
Yufei Xue
drxueyufei@qq.com
[1]Key Laboratory of Sichuan Province for Bamboo Pests Control and Resource Development, Leshan Normal University, Leshan, China
[2]College of Agronomy and Biotechnology, Southwest University, Chongqing, China
[3]College of Tourism and Geographical Science, Leshan Normal University, Leshan, China

Introduction

Bamboo, a perennial evergreen plant of the subfamily Bambooaceae of the Poaceae family, is an extremely important non-wood renewable forestry resources, which also is an important plant for landscaping and has high economical, ecological, and culture values [1, 2]. Most large bamboos, including moso bamboo, are suitable for growing in tropical and subtropical regions, and environment factors such as cold, drought and salt mainly restrict their growth and geographic distribution [3]. Therefore, it is of extreme importance to explore and identify stress-tolerant genes for improving the adaptability of bamboo to abiotic stress through genetic engineering.

Plants have evolved numerous mechanisms to tolerate adverse environments such as low temperature, salt, and drought [4]. Plant fatty acid desaturases (FADs) are responsible for FA desaturations, which catalyze the generation of unsaturated FAs (UFAs) including polyunsaturated FAs (PUFAs) [5]. FA desaturation in membrane lipids can affect the membrane fluidity under abiotic stresses, which contribute to maintaining the structural and functional integrity of cell membranes, and preventing membrane hardening and damage [6]. In addition, PUFAs such as linoleic acid and α-linolenic acid serve as substrates for the biosynthesis of FA-derived signaling molecules including oxylipins and phytohormone JA, in plant responses to abiotic stress [7]. FA desaturation in membrane lipids and PUFA-mediated signaling both play important roles in plant defense against abiotic and biotic stresses [6–9], which are important strategies for surviving adverse environmental conditions.

Nowadays, with the development of society and the advancement of science and technology, reference genomes of more and more plant species have been published [10]. Plant *FAD* genes play essential roles in response to abiotic stresses [6], and thus genome-wide analysis of *FAD* genes under various environment factors has been performed in numerous plants, including wheat [11], rice [12], maize [13], soybean [14], rapeseed [15], cotton [16], banana [17], poplar [18], olive [19], and sunflower [20]. Although reference genomes of moso bamboo have been released [1], there is no report on genome-wide analysis of moso bamboo *FAD* genes (*PeFADs*) under abiotic stresses. The aim of this study is to comprehensively identify the *PeFAD* genes at the whole-genome level, and to mine the potential stress-tolerant *FAD* genes, and then to validate the candidate *PeFAD* gene using the qRT-PCR assay. This work will provide an important molecular basis for the creation of stress-tolerant materials of moso bamboo.

Results

Identification of *PeFAD* genes

We totally identified 43 *PeFAD* genes in moso bamboo genome (Table 1). Gene sequences of *PeFAD* genes ranged from 553 bp to 21,278 bp in length, and their coding regions varied from 351 bp to 1,386 bp in length. PeFAD protein sequences ranged from 116 aa to 461 aa in length. Predicted on SMART database, soluble PeSADs all had FA_desaturase 2 (PF03405) domain, membrane-bound PeFAD4s all contained TMEM189_B domain (PF10520), and other membrane-bound PeFADs all included FA_desaturase domain (PF00487). Theoretical *MW*s of PeFAD proteins varied from 12.79 kDa to 51.08 kDa, and their theoretical *pI* values ranged from 4.57 to 9.71. Predicted on Plant-mPLoc and ProtComp 9.0 databases, PeFAD proteins were mainly localized in chloroplast and endoplasmic reticulum (Supplementary Table 1).

Phylogenetic relationship analysis

In total, 87 FAD proteins from *P. edulis*, *O. sativa* and *A. thaliana*, were utilized to produce the phylogenetic tree. The evolutionary relationship analysis indicated that these 87 FAD proteins were classified into seven groups: SAD/FAB2, DES1, SLD, ADS/FAD5, FAD4, ω-6 and ω-3 (Fig. 1). As shown in Table 2, ADS/FAD5 group only existed in *A. thaliana*, while it was absence both in *P. edulis*, *O. sativa*. The remaining six groups all existed in these three species. In moso bamboo, soluble SAD/FAB2 group contained 25 members, DES1, FAD4 and ω-6 groups both had 3, SLD group harbored 2, ω-3 group contained 7.

Analysis of gene structure and conserved motifs

To analyze gene structures of *PeFAD* genes, their exon-intron organizations were visualized on TBtools program based on the GFF3 file of reference genome (Fig. 2). Among 43 *PeFAD* genes, 2 had no intron, i.e., *PeSAD1* and *PeSLD1*. The remaining 41 *PeFAD* genes harbored 1 (e.g., *PeSAD2*, *PeFAD2.1* and *PeFAD4.1*) to 9 (*PeFAD6* and *PeFAD7.2*) introns. As shown in Table 1, 19 soluble PeFADs contained 2 conserved histidine-motifs, whereas 15 membrane-bound PeFADs had 3 conserved histidine-motifs, which play vital roles in maintaining the catalytic activity of desaturases. The remaining soluble PeFADs (PeSAD3, PeSAD7, PeSAD8, PeSAD10, PeSAD15 and PeSAD25) and membrane-bound PeFADs (PeFAD8.1, PeFAD4.2 and PeFAD4.3) all harbored 1 histidine-boxes, which belong to partial genes and should have no catalytic activity.

Chromosome location and gene duplication analysis

In total, 43 *PeFADs* were unevenly located in 17 hic_scaffolds, in which each hic_scaffold had 1–12

Table 1 The basic information for *PeFAD* genes identified in this study

No.	Gene name	Gene ID	Chromosome ID	Start	End	Strand	Gene length (bp)	CDS length (bp)	Protein length (aa)	Molecular weight	Theoretical *pI*	Histidine mitif 1	Histidine motif 2	Histidine motif 3	CDS types	Conseved domain (SMART)
1	PeSAD1	PH02Gene19500	hic_scaffold_6	76,326,969	76,328,496	-	1528	1233	410	45375.91	8.01	EENRHG	DEKRHE	N/A	Complete	FA_desaturase_2 (PF03405)
2	PeSAD2	PH02Gene12257	hic_scaffold_13	45,053,379	45,054,600	+	1222	1080	359	40816.3	5.69	EENRHG	DEKRHE	N/A	Complete	FA_desaturase_2 (PF03405)
3	PeSAD3	PH02Gene12258	hic_scaffold_13	45,085,715	45,088,532	+	2818	696	231	25455.56	4.57	EENRHG	N/A	N/A	Partial	FA_desaturase_2 (PF03405)
4	PeSAD4	PH02Gene12259	hic_scaffold_13	45,105,263	45,108,251	+	2989	1233	410	46141.57	6.29	EENRHG	DEKRHE	N/A	Complete	FA_desaturase_2 (PF03405)
5	PeSAD5	PH02Gene12260	hic_scaffold_13	45,137,004	45,138,246	+	1243	987	328	36967.85	6.04	EENRHG	DEKRHE	N/A	Complete	FA_desaturase_2 (PF03405)
6	PeSAD6	PH02Gene12261	hic_scaffold_13	45,164,684	45,167,027	+	2344	1239	412	46485.12	7.15	EENRHG	DEKRHE	N/A	Complete	FA_desaturase_2 (PF03405)
7	PeSAD7	PH02Gene31589	hic_scaffold_13	45,214,613	45,215,578	+	966	498	165	18814.54	5.94	EENRHG	N/A	N/A	Partial	FA_desaturase_2 (PF03405)
8	PeSAD8	PH02Gene31588	hic_scaffold_13	45,220,073	45,220,819	+	747	351	116	12787.71	7.83	N/A	DEKRHE	N/A	Partial	FA_desaturase_2 (PF03405)
9	PeSAD9	PH02Gene31586	hic_scaffold_13	45,250,910	45,254,174	-	3265	1260	419	47425.09	6.45	EENRHG	DEKRHE	N/A	Complete	FA_desaturase_2 (PF03405)
10	PeSAD10	PH02Gene31584	hic_scaffold_13	45,303,149	45,303,701	-	553	474	157	18307.87	9.5	EENRHG	N/A	N/A	Partial	FA_desaturase_2 (PF03405)
11	PeSAD11	PH02Gene12263	hic_scaffold_13	45,324,512	45,325,670	+	1159	1011	336	38142.16	5.29	EENRHG	DEKRHE	N/A	Complete	FA_desaturase_2 (PF03405)
12	PeSAD12	PH02Gene07862	hic_scaffold_14	75,138,201	75,139,990	+	1790	1137	378	42764.87	7.19	EENRHG	DEKRHE	N/A	Complete	FA_desaturase_2 (PF03405)
13	PeSAD13	PH02Gene07237	hic_scaffold_14	80,439,738	80,444,570	-	4833	1200	399	45254.49	6.33	EENRHG	DEKRHE	N/A	Complete	FA_desaturase_2 (PF03405)
14	PeSAD14	PH02Gene20845	hic_scaffold_15	29,521,868	29,525,430	+	3563	741	246	27295.37	6.24	EGKRHY	DERRHE	N/A	Complete	FA_desaturase_2 (PF03405)
15	PeSAD15	PH02Gene15757	hic_scaffold_15	95,578,546	95,579,542	+	997	687	228	26169.23	8.7	N/A	DEKRHE	N/A	Partial	FA_desaturase_2 (PF03405)
16	PeSAD16	PH02Gene05757	hic_scaffold_16	7,947,088	7,950,134	+	3047	1200	399	45290.61	6.43	EENRHG	DEKRHE	N/A	Complete	FA_desaturase_2 (PF03405)
17	PeSAD17	PH02Gene40771	hic_scaffold_17	54,111,263	54,116,359	+	5097	1188	395	45041.32	6.48	EENRHG	DEKRHE	N/A	Complete	FA_desaturase_2 (PF03405)
18	PeSAD18	PH02Gene36679	hic_scaffold_20	4,886,972	4,890,271	+	3300	1188	395	44710.03	6.42	EENRHG	DEKRHE	N/A	Complete	FA_desaturase_2 (PF03405)
19	PeSAD19	PH02Gene46704	hic_scaffold_21	53,781,875	53,784,182	+	2308	1287	428	46657.29	7.22	EENRHG	DERRHE	N/A	Complete	FA_desaturase_2 (PF03405)

Table 1 (continued)

No.	Gene name	Gene ID	Chromosome ID	Start	End	Strand	Gene length (bp)	CDS length (bp)	Protein length (aa)	Molecular weight	Theoretical *pI*	Histidine mitif 1	Histidine motif 2	Histidine motif 3	CDS types	Conseved domain (SMART)
20	PeSAD20	PH02Gene14299	hic_scaffold_23	48,366,094	48,370,535	+	4442	1185	394	44956.12	7.13	EENRHG	DEKRHE	N/A	Complete	FA_desaturase_2 (PF03405)
21	PeSAD21	PH02Gene44797	hic_scaffold_23	73,114,501	73,115,835	+	1335	1218	405	44938.25	8.43	EENRHG	DEKRHE	N/A	Complete	FA_desaturase_2 (PF03405)
22	PeSAD22	PH02Gene41206	hic_scaffold_23	73,123,140	73,125,194	+	2055	1236	411	46134.48	7.19	EENRHG	DEKRHE	N/A	Complete	FA_desaturase_2 (PF03405)
23	PeSAD23	PH02Gene41208	hic_scaffold_23	73,151,331	73,152,665	-	1335	1218	405	44968.27	8.43	EENRHG	DEKRHE	N/A	Complete	FA_desaturase_2 (PF03405)
24	PeSAD24	PH02Gene28642	hic_scaffold_24	26,003,718	26,009,357	-	5640	1182	393	44880.99	8.22	EENRHG	DEKRHE	N/A	Complete	FA_desaturase_2 (PF03405)
25	PeSAD25	PH02Gene24080	hic_scaffold_2757	81,719	82,673	-	955	477	158	17749.3	5.83	N/A	DEKCHG	N/A	Partial	FA_desaturase_2 (PF03405)
26	PeFAD2.1	PH02Gene22841	hic_scaffold_3	88,491,036	88,496,439	-	5404	1167	388	44307.1	8.45	HECGHH	HRRHH	HVAHH	Complete	FA_desaturase (PF00487)
27	PeFAD2.2	PH02Gene16801	hic_scaffold_17	16,604,581	16,609,362	+	4782	1161	386	44077.92	8.63	HECGHH	HRRHH	HVAHH	Complete	FA_desaturase (PF00487)
28	PeFAD6	PH02Gene20531	hic_scaffold_13	64,242,752	64,248,094	+	5343	1329	442	50969.26	9.18	HDCAH	HDRHH	HVPHH	Complete	FA_desaturase (PF00487)
29	PeFAD3.1	PH02Gene44248	hic_scaffold_2	28,553,924	28,575,201	-	21,278	1194	397	45371.84	8.4	HDCGH	HRIHH	HVIHH	Complete	FA_desaturase (PF00487)
30	PeFAD3.2	PH02Gene44250	hic_scaffold_2	28,609,938	28,630,686	-	20,749	1194	397	45325.92	8.58	HDCGH	HRIHH	HVIHH	Complete	FA_desaturase (PF00487)
31	PeFAD3.3	PH02Gene21566	hic_scaffold_13	349,596	353,537	-	3942	1176	391	44943.39	8.93	HDCGH	HRTHH	HVIHH	Complete	FA_desaturase (PF00487)
32	PeFAD7.1	PH02Gene00068	hic_scaffold_15	51,724,798	51,728,190	+	3393	1347	448	50207.64	8.97	HDCGH	HRTHH	HVIHH	Complete	FA_desaturase (PF00487)
33	PeFAD7.2	PH02Gene23551	hic_scaffold_21	82,848,094	82,850,856	+	2763	1218	405	45608.43	8.99	HDCGH	HRTHH	HVIHH	Complete	FA_desaturase (PF00487)
34	PeFAD8.2	PH02Gene16646	hic_scaffold_4	380,222	383,958	-	3737	1275	424	48000.08	8.86	HDCGH	HRTHH	HVIHH	Complete	FA_desaturase (PF00487)
35	PeFAD8.1	PH02Gene13663	hic_scaffold_2	28,512,939	28,523,496	-	10,558	450	149	17299.8	9.71	N/A	N/A	HVIHH	Partial	FA_desaturase (PF00487)
36	PeFAD4.1	PH02Gene39556	hic_scaffold_18	19,787,694	19,789,046	+	1353	876	291	31284.38	9.09	FQGHHR	HSWAH	HAAHH	Complete	TMEM189_B_ dmain (PF10520)
37	PeFAD4.2	PH02Gene24139	hic_scaffold_22	48,180,260	48,181,155	-	896	615	204	21878.7	6.36	N/A	N/A	HAAHH	Partial	TMEM189_B_ dmain (PF10520)
38	PeFAD4.3	PH02Gene39558	hic_scaffold_18	19,834,563	19,835,264	+	702	513	170	18359.85	4.92	FQGHHR	N/A	N/A	Partial	TMEM189_B_ dmain (PF10520)

Table 1 (continued)

No.	Gene name	Gene ID	Chromosome ID	Start	End	Strand	Gene length (bp)	CDS length (bp)	Protein length (aa)	Molecular weight	Theoretical *pI*	Histicitif 1	Histidine motif 2	Histidine motif 3	CDS types	Conseved domain (SMART)
39	PeDES1.1	PH02Gene40570	hic_scaffold_3	74,351,567	74,357,270	+	5704	987	328	37967.77	8.79	HELSH	HLEHH	HNEHH	Complete	FA_desaturase (PF00487)
40	PeDES1.2	PH02Gene16913	hic_scaffold_17	29,332,269	29,335,436	-	3168	981	326	37593.39	8.5	HELSH	HLEHH	HNEHH	Complete	FA_desaturase (PF00487)
41	PeDES1.3	PH02Gene02088	hic_scaffold_24	51,356,905	51,360,358	+	3454	987	328	37783.66	8.77	HELSH	HLEHH	HNEHH	Complete	FA_desaturase (PF00487)
42	PeSLD1	PH02Gene30788	hic_scaffold_3	33,818,104	33,820,342	-	2239	1386	461	51077.84	8.53	HDSGHH	HNTHH	QIEHH	Complete	FA_desaturase (PF00487)
43	PeSLD2	PH02Gene31223	hic_scaffold_19	5,531,353	5,532,717	-	1365	1248	415	46608.5	8.87	HDSGHH	HNTHH	QIEHH	Complete	FA_desaturase (PF00487)

PeFADs (Table 1). The hic_scaffold_13 harbored 12, hic_scaffold_23 had 4, hic_scaffold_15, hic_scaffold_17, hic_scaffold_2 and hic_scaffold_3 all contained 3, hic_scaffold_14, hic_scaffold_18, hic_scaffold_21 and hic_scaffold_24 all included 2, and hic_scaffold_16, hic_scaffold_19, hic_scaffold_20, hic_scaffold_22, hic_scaffold_4, hic_scaffold_6 and hic_scaffold_2757 all possessed 1. Gene duplication analysis indicated that 46 duplicated gene pairs were identified in 43 *PeFAD* genes (Table 3), in which 34 gene pairs (73.91%; composed of *PeSADs*, *PeFAD2s*, *PeFAD3s*, *PeFAD7s*, *PeDES1s* and *PeSLD1s*) were segmental duplication type and the rest 12 (26.09%; consisting of *PeSADs* and *PeFAD3s*) were tandem duplication type. Of 34 segmental duplications, 26 (76.47%) belonged to *PeSADs*, whereas among 12 tandem duplications, 11 (91.67%) were *PeSADs*. To examine the selection pressures for duplicated gene pairs, the *Ka* and *Ks* values were computed (Table 3). For 46 duplicated gene pairs, only 1 contained a *Ka/Ks* ratio of more than 1, and the lest all had the *Ka/Ks* ratios with less than 1, revealing that there mainly occurred purifying selection in their evolution process.

Prediction of miRNAs targeting *PeFAD* genes

The miRNAs play important roles in gene post-transcription regulation, and thus the miRNAs targeting *PeFAD* genes were predicted. As shown in Supplementary Table 2, there existed a total of 59 types of miRNAs for targeting 22 *PeFAD* genes, and their regulation types all belonged to the cleavage effect. There were 37 miRNAs, which all targeted *PeFAD3.3* gene, and 6 miRNAs all for *PeFAD4.1* gene, whereas *PeFAD8*.2, *PeFAD2*.2, *PeFAD2*.1, *PeFAD7*.2, *PeSAD18* and *PeSAD10* all had 2 miRNAs, and the remaining 14 *PeFAD* genes all contained only 1 miRNA. This showed that these identified miRNAs might participate in gene post-transcription regulations of corresponding *PeFAD* genes.

Expression of *PeFAD* genes in different organs/tissues

To detect the potential biological function of 34 full-length *PeFAD* genes with complete histidine-boxes, we analyzed their expression patterns in 19 different tissues/organs based on published RNA-seq data (Supplementary Table 3), including roots, lateral buds, rhizome tips, shoot tips, 0.2–7.0 m shoots, inflorescences, seedling leaves, one-year leaves, next-year flower leaves, flower leaves, flower florets, and germination seeds. In total, transcriptomic data of these 34 *PeFADs* all were obtained (Fig. 3; Supplementary Table 4), in which 4 (*PeSAD17*, *PeSAD5*, *PeSAD11* and *PeSAD14*) almost had no expression in all tissues (their TPM values all were <1), and the remaining 30 *PeFADs* were expressed in various tissues/organs with the different levels. The TPM values of *PeSAD1* were >1 only in germination seeds (1.42), and

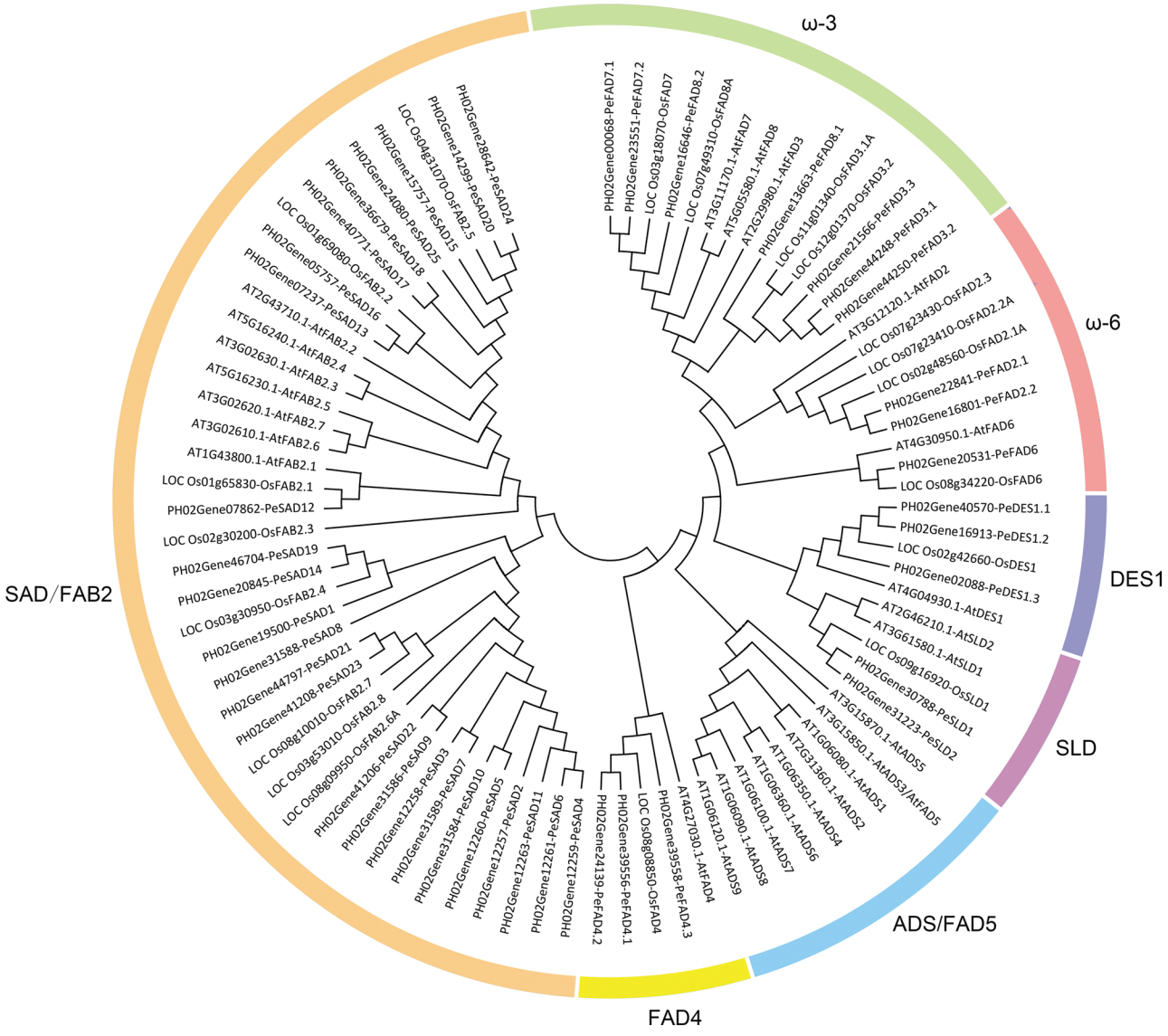

Fig. 1 Phylogenetic tree of FAD proteins among *P. edulis*, *O. sativa* and *A. thaliana*

Table 2 The total number of *FAD* genes within each group in *P. edulis*, *O. sativa* and *A. thaliana*

Category	*P.* edulis	O. sativa	A. thaliana
Total	43	19	25
Total Soluble FADs	25	8	7
SAD/FAB2	25	8	7
Total Membrane FADs	18	11	18
DES1	3	1	1
SLD	2	1	2
ADS/FAD5	0	0	9
FAD4	3	1	1
ω-6	3	4	2
ω-3	7	4	3

PeSAD2 was only in flower florets and inflorescences. *PeFAD3.1*, *PeFAD3.2* and *PeSAD21* both had higher expression levels in 0.5–3.0 m shoots than other organs/tissues. *PeSAD4* and *PeSAD6* both were expressed in flower florets with higher levels than other organs/tissues. *PeFAD2.2*, *PeSAD16*, *PeSAD13*, *PeFAD2.1*, *PeSAD24*, and *PeSLD1* all had constitutively high expression with the TPM values of 8.13-162.72. *PeFAD3.3*, *PeDES1.2*, *PeDES1.3* and *PeDES1.1* contained high expression levels in rhizome tips, shoot tips, 0.2–6.0 m shoots and flower florets. This result showed that *PeFAD* genes might have important roles in growth and development of moso bamboo.

Fig. 2 Gene structure of *PeFAD* genes in *P. edulis*

Expression of *PeFAD* genes in response to abiotic stresses and hormone treatments

To analyze important roles of 34 full-length *PeFAD* genes in plant stress responses, and thus we detected their expression patterns in response to drought, salt, cold, SA, ABA, BR, NAA and GA treatments using published transcriptome data (Supplementary Tables 5–9). Under PEG treatment (Fig. 4a), there existed 2 up-regulated *PeFAD* DEGs (*PeFAD7.1* and *PeSAD6*) and 6 down-regulated DEGs at 3 h, whereas 2 up-regulated DEGs (*PeSAD5* and *PeSAD11*) and 4 down-regulated DEGs were obtained at 24 h. Under NaCl treatment (Fig. 4a), we detected 6 up-regulated DEGs (*PeSAD11*, *PeFAD7.1*, *PeSAD4*, *PeSAD9*, *PeFAD2.1*, *PeSAD6*) and 1 down-regulated DEGs at 3 h, and there were 1 up-regulated DEGs (*PeFAD2.1*) and 7 down-regulated DEGs at 24 h. Under SA treatment (Fig. 4a), 1 up-regulated DEGs (*PeFAD7.1*) and 6 down-regulated DEGs were observed at 3 h, whereas there existed 4 up-regulated DEGs (*PeSAD11*, *PeSAD5*, *PeFAD2.1*, and *PeSAD4*) and 6 down-regulated DEGs at 24 h. Under ABA treatment (Fig. 4a), we detected 5 up-regulated DEGs (*PeSAD4*, *PeSAD9*, *PeFAD2.1*, *PeFAD3.3*, and *PeSAD6*) and 6 down-regulated DEGs at 3 h, whereas there were 7 DEGs at 24 h, which all were down-regulated. Under the treatment of PPZ with/without BR (Fig. 4b), a total of 5 up-regulated DEGs and 3 down-regulated DEGs (*PeDES1.2*, *PeFAD3.2*, and *PeFAD3.3*) for PPZ-responsive genes in shoot and root parts, whereas there were 2 up-regulated DEGs (*PeSAD12* and *PeDES1.2*) and 1 down-regulated DEGs for BR-responsive genes in these two parts. There existed a total of 4 NAA-responsive *PeFAD* DEGs (*PeSLD2*, *PeDES1.3*, *PeFAD3.3* and *PeFAD3.2*), whose expression levels all were decreased upon NAA treatment (Fig. 4c). In response to GA treatment, there only existed 4 up-regulated *PeDAD* DEGs (*PeSAD23*, *PeSAD9*, *PeSAD4* and

Table 3 Gene duplication types and *Ka/Ks* analysis for duplicated gene pairs of *PeFADs*

No.	Gene_1	Gene_2	*Ka*	*Ks*	*Ka/Ks*	Duplication type
1	*PeSAD5*	*PeSAD2*	0.1219	0.1579	0.7719	Tandem duplication
2	*PeSAD5*	*PeSAD6*	0.1170	0.1303	0.8980	Tandem duplication
3	*PeSAD5*	*PeSAD4*	0.1321	0.1765	0.7485	Tandem duplication
4	*PeSAD5*	*PeSAD11*	0.1148	0.1874	0.6124	Tandem duplication
5	*PeSAD9*	*PeSAD5*	0.1751	0.2581	0.6787	Tandem duplication
6	*PeSAD9*	*PeSAD2*	0.0713	0.1537	0.4638	Tandem duplication
7	*PeSAD9*	*PeSAD6*	0.0610	0.1629	0.3749	Tandem duplication
8	*PeSAD9*	*PeSAD4*	0.0579	0.1555	0.3722	Tandem duplication
9	*PeSAD9*	*PeSAD11*	0.0600	0.1822	0.3293	Tandem duplication
10	*PeSAD13*	*PeSAD16*	0.0204	0.1219	0.1677	Segmental duplication
11	*PeSAD14*	*PeSAD19*	0.1150	0.2381	0.4832	Segmental duplication
12	*PeSAD17*	*PeSAD18*	0.0395	0.2908	0.1358	Segmental duplication
13	*PeSAD17*	*PeSAD24*	0.0825	0.8448	0.0977	Segmental duplication
14	*PeSAD17*	*PeSAD20*	0.0921	0.8861	0.1039	Segmental duplication
15	*PeSAD18*	*PeSAD20*	0.0948	0.8397	0.1130	Segmental duplication
16	*PeSAD18*	*PeSAD24*	0.0880	0.7487	0.1175	Segmental duplication
17	*PeSAD20*	*PeSAD24*	0.0169	0.1198	0.1409	Segmental duplication
18	*PeSAD21*	*PeSAD22*	0.1231	0.2220	0.5543	Tandem duplication
19	*PeSAD21*	*PeSAD9*	0.1190	0.2188	0.5436	Segmental duplication
20	*PeSAD21*	*PeSAD5*	0.2383	0.3513	0.6783	Segmental duplication
21	*PeSAD21*	*PeSAD2*	0.1397	0.2778	0.5027	Segmental duplication
22	*PeSAD21*	*PeSAD6*	0.1483	0.2754	0.5383	Segmental duplication
23	*PeSAD21*	*PeSAD4*	0.1530	0.3029	0.5050	Segmental duplication
24	*PeSAD21*	*PeSAD11*	0.1417	0.2971	0.4768	Segmental duplication
25	*PeSAD22*	*PeSAD9*	0.0737	0.1444	0.5106	Segmental duplication
26	*PeSAD22*	*PeSAD5*	0.2245	0.3072	0.7309	Segmental duplication
27	*PeSAD22*	*PeSAD2*	0.1218	0.2054	0.5933	Segmental duplication
28	*PeSAD22*	*PeSAD6*	0.1161	0.2030	0.5721	Segmental duplication
29	*PeSAD22*	*PeSAD4*	0.1124	0.2146	0.5239	Segmental duplication
30	*PeSAD22*	*PeSAD11*	0.1129	0.2305	0.4899	Segmental duplication
31	*PeSAD23*	*PeSAD22*	0.1244	0.2220	0.5603	Tandem duplication
32	*PeSAD23*	*PeSAD9*	0.1190	0.2188	0.5436	Segmental duplication
33	*PeSAD23*	*PeSAD5*	0.2383	0.3513	0.6783	Segmental duplication
34	*PeSAD23*	*PeSAD2*	0.1397	0.2778	0.5027	Segmental duplication
35	*PeSAD23*	*PeSAD6*	0.1496	0.2754	0.5433	Segmental duplication
36	*PeSAD23*	*PeSAD4*	0.1544	0.3029	0.5095	Segmental duplication
37	*PeSAD23*	*PeSAD11*	0.1417	0.2971	0.4768	Segmental duplication
38	*PeFAD2.1*	*PeFAD2.2*	0.0116	0.0872	0.1335	Segmental duplication
39	*PeFAD3.1*	*PeFAD3.2*	0.0196	0.0124	1.5804	Tandem duplication
40	*PeFAD3.1*	*PeFAD3.3*	0.0548	0.1697	0.3227	Segmental duplication
41	*PeFAD3.2*	*PeFAD3.3*	0.0687	0.1683	0.4082	Segmental duplication
42	*PeFAD7.1*	*PeFAD7.2*	0.0426	0.1950	0.2184	Segmental duplication
43	*PeDES1.1*	*PeDES1.2*	0.0175	0.0939	0.1864	Segmental duplication
44	*PeDES1.1*	*PeDES1.3*	0.0465	0.6322	0.0735	Segmental duplication
45	*PeDES1.2*	*PeDES1.3*	0.0446	0.6555	0.0681	Segmental duplication
46	*PeSLD1*	*PeSLD2*	0.0371	0.1967	0.1887	Segmental duplication

PeSAD6) (Fig. 4d). Under cold treatment (Fig. 5a), there existed only 2 cold-responsive DEGs (both up-regulated), *PeSLD1* and *PeSAD4*, in which expression levels and change-folds of *PeSLD1* both were higher than *PeSAD4*. This result suggested that *PeSLD1* might play a more important role in cold response and tolerance.

Validation of cold-responsive *PeSLD1* gene and analysis of its upstream regulatory gene

Top cold-responsive gene *PeSLD1* was selected to perform the qRT-PCR assay for validating the accuracy of transcriptome results. Results showed that the expression levels of *PeSLD1* were significantly up-regulated

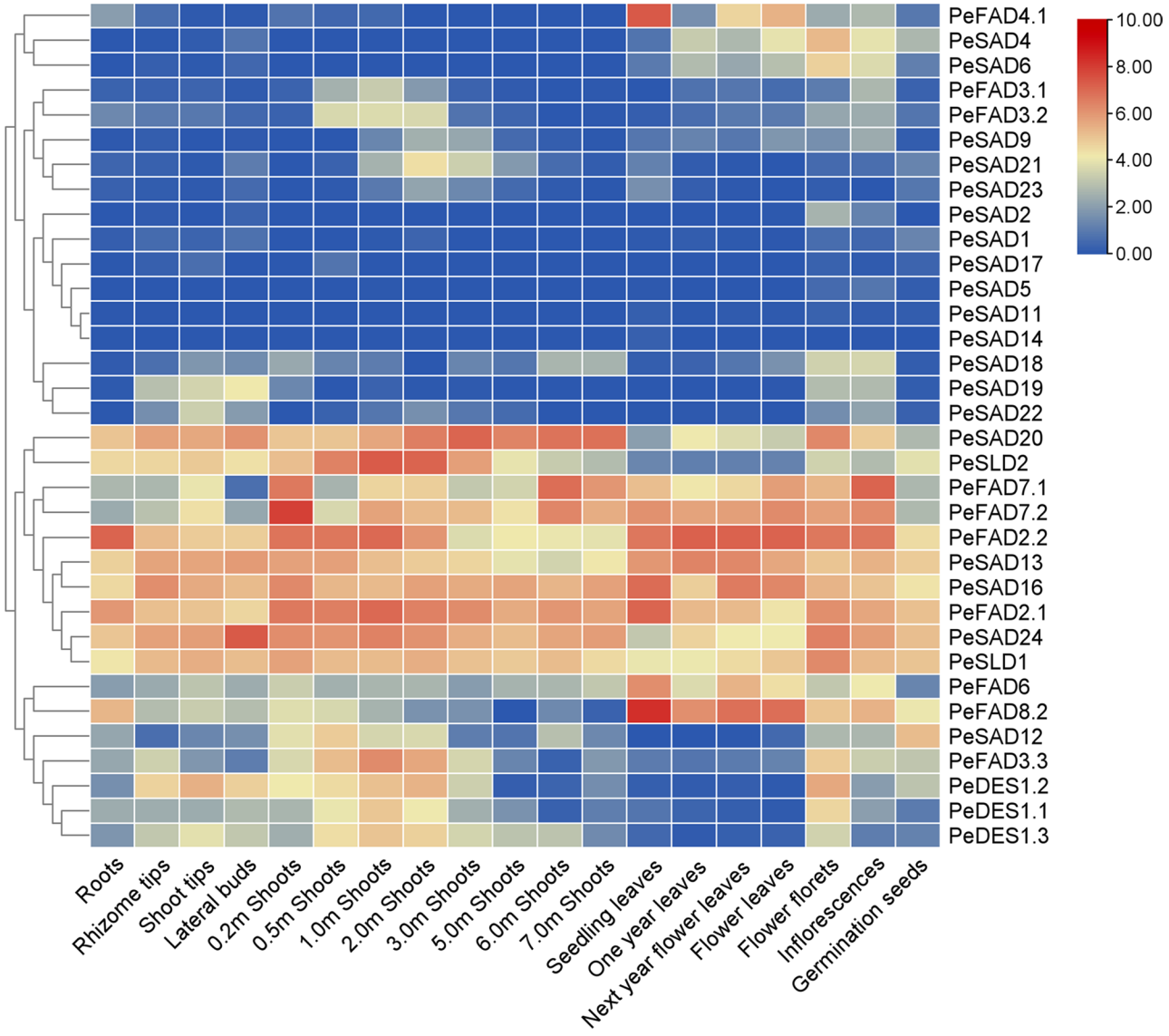

Fig. 3 Expression patterns of *PeFAD* genes in 19 different tissues/organs

after cold treatment (Fig. 6c). *cis*-Element analysis of *PeSLD1* promoter showed that there existed low-temperature responsiveness (LTR)-element and DRE core element in its promoter. Plant AP2/ERF proteins can bind to DNA sequences of DRE core element, and are also involved in regulating plant cold tolerance, such as CBF1, CBF2 and CBF3 [21]. To mine potential AP2/ERF family member that regulates *PeSLD1* expression, we performed co-expression analysis of *PeSLD1* with all AP2/ERF family genes under cold stress in moso bamboo (Fig. 5b; Supplementary Table 10). Results showed that there were a cold-responsive cluster, in which *PeSLD1* clustered with 15 *AP2/ERF* genes. *PeCBF3* is the top cold-responsive gene among these 15 *AP2/ERF* candidates (Fig. 5c). The qRT-PCR assay also validated the cold inducibility of *PeCBF3* (Fig. 6c), suggesting that *PeCBF3* might directly target *PeSLD1* promoter. The regulatory effect of upstream gene *PeCBF3* on *PeSLD1* is worth being confirmed with protein-DNA interaction experiments. Additionally, the difference of chlorophyll fluorescence parameters of moso bamboo leaves after cold stress compared with the control were analyzed by plant phenotype imager. Results indicated that chlorophyll fluorescence parameters, *NPQ*, Φ_{PSII} and *Fv/Fm* varied after cold treatment (Fig. 6a, b), suggesting the potential application of this device in screening of cold-tolerant germplasm materials of bamboo.

Discussion

Bamboo is an extremely important non-wood renewable forestry resource with high economical, ecological, and culture values. Nowadays, numerous environmental

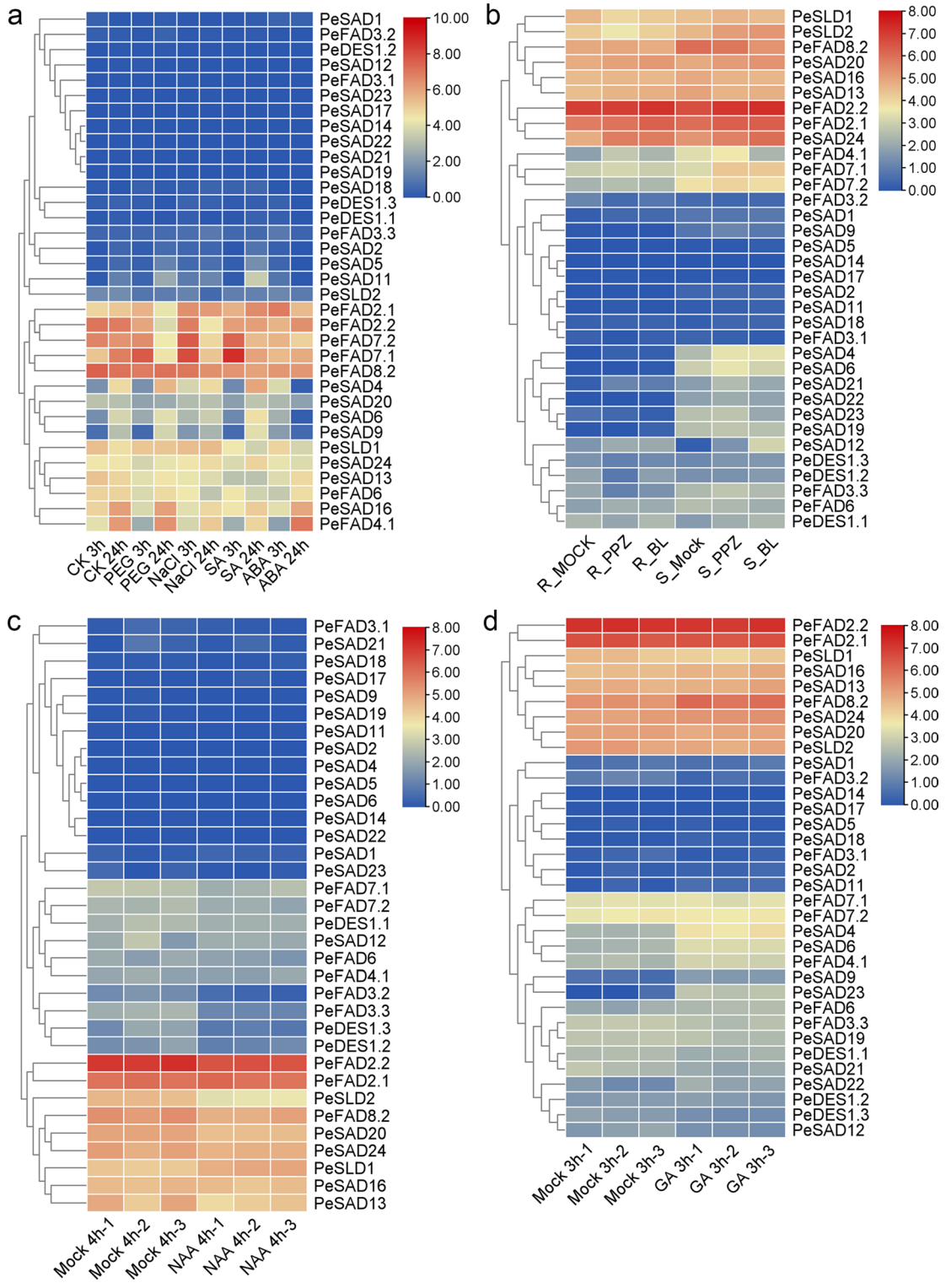

Fig. 4 Expression patterns of *PeFAD* genes under the treatment of salt and drought stresses, and plant hormones. **a**, PEG, NaCl, SA and ABA; **b**, PPZ and BL (BR); **c**, NAA; **d**, GA

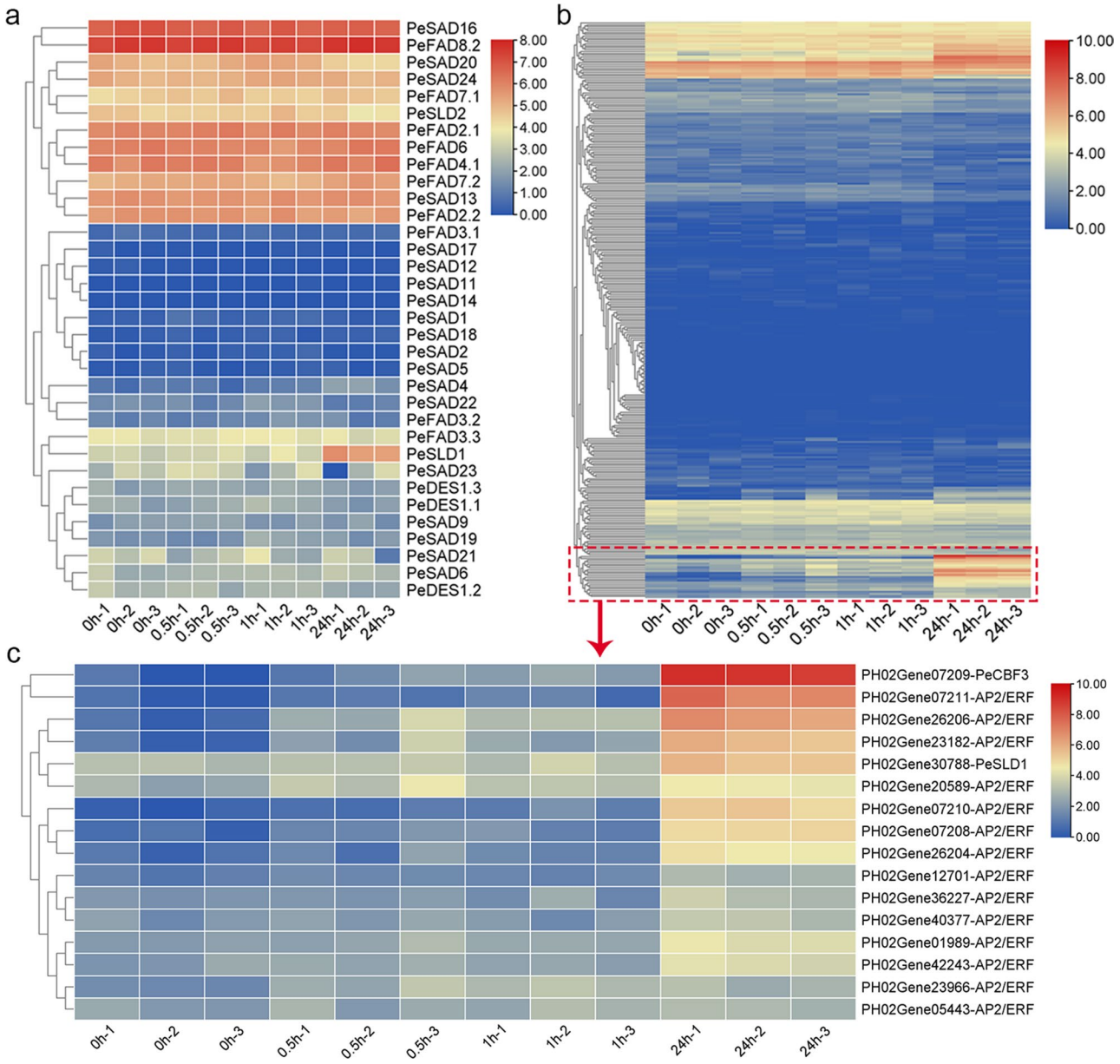

Fig. 5 Expression patterns of *PeFAD* genes under cold stress (a) and co-expression of top cold-responsive *PeSLD1* and potential upstream regulatory AP2-ERFs (**b** and **c**)

factors such as low temperature, drought, and salinity severely restricted bamboo growth, development, and geographic distribution. Plant *FAD* genes play important roles in defense against abiotic stresses by regulating the FA desaturation in cell membrane, and FA-mediated signaling transduction. Although reference genomes of various bamboo species have been sequenced, the information of comprehensive analysis of bamboo *FAD* genes upon abiotic stresses at whole-genome level is limited. In this study, we performed a systemically genome-wide analysis of moso bamoo *PeFAD* genes under abiotic stresses and phytohormone treatments, and identified substantial abiotic stress-responsive *PeFAD* genes, which is of great importance for creating stress-tolerant bamboo cultivar using genetic engineering.

A total of 43 *PeFAD* genes were identified in moso bamboo genome. There existed 46 duplicated gene pairs, which contained 34 segmental duplications and 12 tandem duplications. Gene duplication analysis showed that diversity and expansion of *PeFAD* genes mainly resulted from segmental duplications (76.47%, 26/34) and tandem duplications (91.67%, 11/12) of *PeSAD* group. Gene expansion of chia *FAD* genes also mainly resulted from gene duplications of ShSAD group, but it all belonged to tandem duplication type [22]. Moreover, the *Ka/Ks* ratios of duplicated gene pairs of *PeFADs* were less than

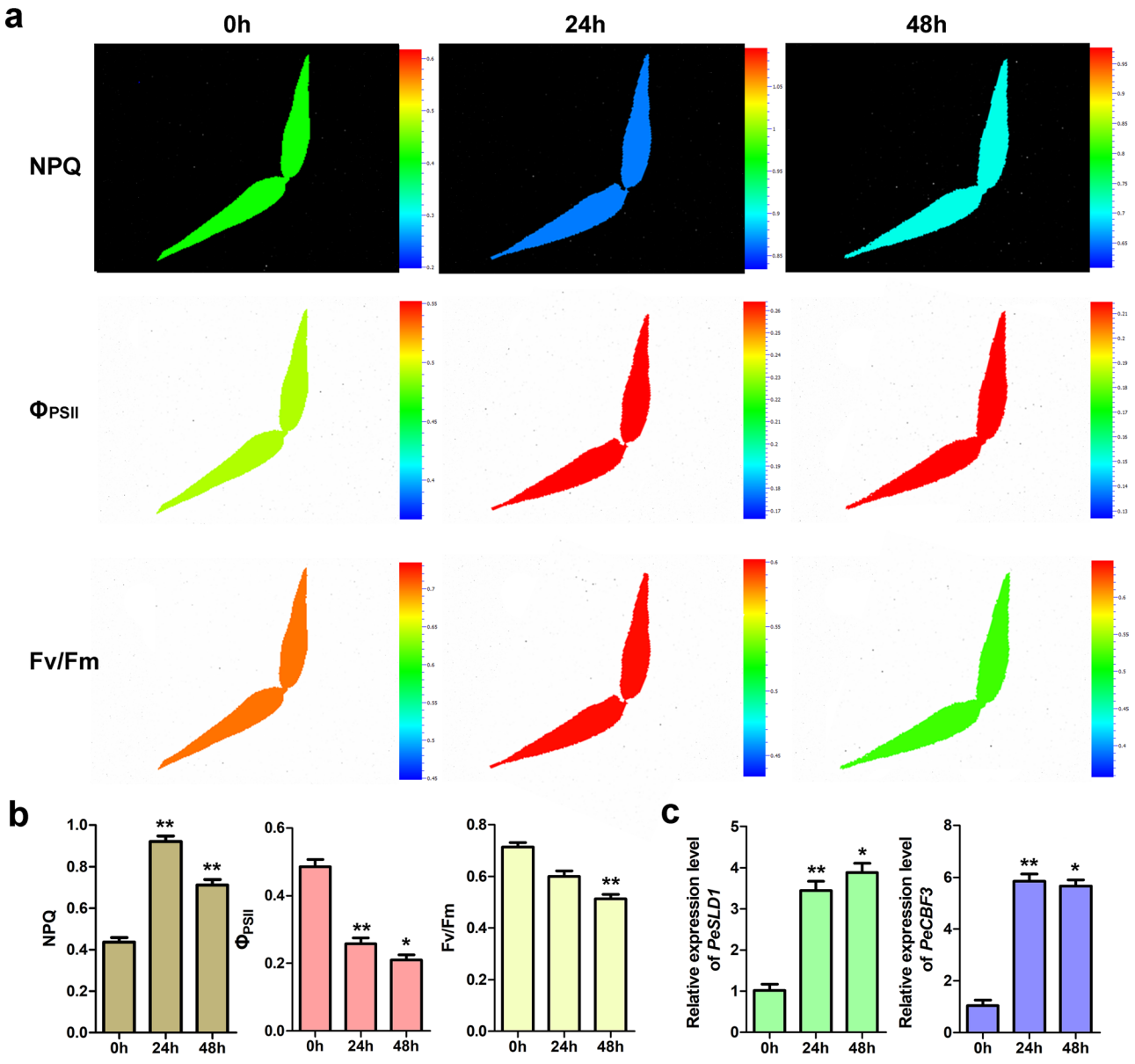

Fig. 6 The impact of cold stress on photosynthesis of moso bamboo leaves (**a**, **b**), and the qRT-PCR expression level of top cold-responsive gene *PeSLD1* and its potential upstream regulatory gene *PeCBF3*, (**c**). Standard images of the *Fv/Fm*, Φ_{PSII} and *NPQ* from cold-treated moso bamboo leaves at 0, 24 and 48 h. A false color scale is used for each parameter. The values represent the average ± SD of 3 biological replicates. *Fv/Fm*, maximum quantum yield of *PSII*; Φ_{PSII}, effective quantum yield of *PSII*; *NPQ*, non-photochemical quenching. * $p < 0.05$ and ** $p < 0.01$ compared with samples at 0 h

1 except for *PeFAD3.1*/*PeFAD3.2*, revealing that they mainly subjected to negative selection in evolution process, which was similar with those of banana [17], poplar [18], and sunflower [20].

Phylogenetic relationship analysis revealed that *ADS/FAD5* gene group was absent in moso bamboo and rice, but Arabidopsis contained this group. This phenomenon also occurred in banana, barley, wheat, and maize, while there also existed *ADS/FAD5* group in wheat [11], soybean [14], cotton [16], rapeseed [15], sunflower [20], chia and perilla [22], poplar [18], and camelina [23]. These reports and this study obviously both supported the hypothesis that monocots might lose *ADS/FAD5* group and dicots retained it after separation from the ancestral species, while the functional evolution mechanism need to further be studied and revealed.

Substantial studies have indicated that *FAD* genes play critical roles in plant response to various stresses such as cold, salinity and drought [6]. For example, *ADS2* gene was found to play important roles in chilling and freezing tolerance in Arabidopsis by modulating the FA composition of organelle membrane [24]. *PpSFD* mutants for *Physcomitrium patens SLD* gene exhibited a cold-sensitive phenotype, and *PpSFD* over-expression

in *atads2* mutant could functionally complemented its phenotype, suggesting its important roles in cold tolerance [25]. Tomato *SlSLD* gene also had important roles in plant chilling resistance [26]. Here, we found two cold-responsive genes, *PeSLD1* and *PeSAD6*, in moso bamboo, and cold inducibility of *PeSLD1* was also validated by the qRT-PCR assay, which thus *PeSLD1* had great potential in improving cold tolerance in bamboo. In addition, transgenic soybeans over-expressing *GmFAD3A* possessed the tolerance to drought and salinity stresses, while soybean plants of *GmFAD3* silencing were sensitive to drought and salinity stresses [27]. Arabidopsis *FAD2* gene were involved in plant ER stress [28], and loss-of-function mutant of *FAD2* was sensitive to salt stress [29]. In this study, two *PeFAD* DEGs (*PeFAD7.1* and *PeSAD6*) were also found to be significantly up-regulated both in salt and drought stresses, showing their potential roles in abiotic stress tolerance. Heterogeneous expression of flax *LuSAD1* and *LuSAD2* also enhanced seedling cold and drought tolerance in rapeseed [30].

Plant FADs have been reported to catalyze the UFA production [6], and UFAs such as linoleic acid and linolenic acid are precursors for the biosynthesis of FA-derived signal molecules, including JA, oxylipin, and sphingolipid [25, 31]. JA signaling pathway often occur crosstalk with other phytochrome pathways for regulation of the trade-offs in growth and defense [32, 33]. In this study, there both existed 2 common upregulated *PeFAD* DEGs (*PeFAD2.1* and *PeSAD4*) under SA and ABA treatments. In tomato, *SlFAD2-4* and *SlFAD2-7* were also upregulated by SA, and their expression is independent of JA synthesis [34]. In poplar, *PtFAB2.3*, *PtFAB2.4* and *PtFAB2.5* were also upregulated under ABA treatments [18]. *PeDES1.2* was up-regulated under BR treatment, and down-regulated under BR-inhibitor PPZ treatment. Four up-regulated DEGs were found in response upon GA treatment, respectively, while there only existed 4 down-regulated DEGs under NAA treatments. In rice, most *OsFAD* genes were responsive to GA treatment [12]. In Arabidopsis, auxin and cytokinin treatments upregulated ectopic *FAD3* expression in roots only during vegetative growth [35]. Therefore, plant *FAD* genes play important roles in regulating the synthesis and transduction of plant signal molecules as well as plant defense.

Previous studies indicated that various types of TFs directly targeted plant *FAD* genes. For example, banana MaABI5-like directly targeted *MaFAD3-1*, *MaFAD3-4*, *MaFAD3-5*, *MaFAD6-2*, *MaFAD6-3* and thus could increase plant cold tolerance [36]. The three most highly expressed *SAD* genes in *Arabidopsis* seeds, *FAB2*, *AAD1*, and *AAD5*, were directly activated by the WRI1 TF [37]. In this study, *PeCBF3* binding site (GCCGAC, DRE core) and LTR element was predicted in promoter of top cold-responsive *PeSLD1*. Co-expression and qRT-PCR assay both validated their strong cold inducibility. This result suggests that the expression of *PeSLD1* gene might be directly regulated by PeCBF3, which thus deserves further study.

The miRNAs serve as small endogenous RNAs that alter gene-expression at posttranscriptional level, which exist widely in organism including plants and animals. miRNAs participate in regulating plant growth, development, and defense [38]. In banana, 12 *MaFAD* genes were predicted to be regulated by 30 miRNAs [17]. In peanut, 20 *AhFAD* genes were predicted to be targeted by 19 miRNAs [39]. This study found that 59 types of miRNAs were predicted to target 22 *PeFAD* genes. These *PeAD* genes might be directly regulated by the corresponding predicted miRNAs, which need to be validated in the further study.

For the characterization of plant cold tolerance, it is of quite significance to apply a rapid high-throughput, and non-invasive detection procedure instead of time-consuming and labor-intensive detection means. In this study, we for the first time detected the potential of plant phenotype imager in checking the low temperature response in moso bamboo seedling. Under cold stress, values of three chlorophyll fluorescence parameters, *NPQ*, Φ_{PSII}, and *Fv/Fm*, all altered significantly. There also were similar reports in Arabidopsis and oats [40, 41]. This result suggested that plant phenotype imager had a great potential in measuring cold response of bamboos with an easy and non-invasive method at a large scale.

Conclusion

Here, a systemically whole-genome-wide analysis of *PeFAD* genes were performed in moso bamboo. A total of 43 *PeFAD* genes were identified in moso bamboo, which were mapped in 17 scaffolds. Evolutionary relationship analysis revealed that *PeFAD* genes were classified into 6 groups and there was no ADS/FAD5 group in momo bamboo, and each group remained highly conserved in gene exon-intron organization and protein histidine-motifs. Gene duplication of SAD/FAB2 group mainly resulted in diversity and expansion of *PeFAD* genes. Top cold-responsive gene contained LTR *cis*-element and DRE core element in its promoter. Co-expression analysis and qRT-PCR assay confirmed that PeCBF3 might directly target *PeSLD1*. In total, 59 types of miRNAs were predicted to target *PeFAD* genes. Transcriptome data analysis implied that *PeFAD* genes were differentially expressed in 19 tissues/organs as well as were responsive to abiotic stresses and various phytohormones. This study will provide important references for further functional studies of stress-responsive *PeFAD* genes.

Materials and methods

Sequence retrieval and structural analysis

To identify the *PeFAD* genes, we downloaded the HMM files of FAD domain (PF03405, PF00487 and PF10520) from Pfam database (http://Pfam.sanger.ac.uk/), and then we performed the hmmsearch operation (e-value 10e−5; http://hmmer.org) against moso bamboo genome (http://gigadb.org/dataset/view/id/100498) to obtain PeFAD proteins. Meanwhile, we also perform BlastP to obtain the PeFAD proteins using Arabidopsis FAD (AtFAD) protein sequences as queries. All candidates were checked using SMART database ((http://smart.embl-heidelberg.de/) and SUPERFAMILY 2 database (https://beta.supfam.org/), and non-FADs all were removed. Based on chromosome locations and homology with *AtFAD* genes [15], we determined the names of *PeFAD* genes. We predicted the subcellular location of PeFAD proteins using ProtComp 9.0 (http://www.softberry.com/) and Plant-mPLoc (http://www.csbio.sjtu.edu.cn/bioinf/plant-multi/) websites. We calculated their theoretical isoelectric points (*pI*) and molecular weights using the ProtParam tool (https://web.expasy.org/protparam/).

Phylogenetic relationship analysis

The multiple alignment of the of PeFAD, OsFAD and AtFAD protein sequences [15], were performed using MAFFT7 with the default parameters, and then we generated the phylogenetic tree on MEGA7 software with neighbor-joining (NJ) method using the 1000 bootstrap replicates and *p*-distance model.

Analysis of gene structure and conserved motifs

We analyzed the *PeFAD* gene structures based on GFF3 file of reference genome using TBtools-II [42]. We also analyzed the conserved histidine motifs of PeFAD proteins based on the multiple alignment result of PeFAD proteins, and OsFAD and AtFAD proteins.

Chromosome location, gene duplication and selection pressure analysis

We analyzed the chromosome location information of *PeFAD* genes using GFF3 file of reference genome on TBtools-II. Duplicated gene pairs of *PeFAD* genes were identified as previously described [43]. We calculated the non-synonymous substitution (*Ka*) and synonymous substitution (*Ks*) values of the duplicated gene pairs using simple *Ka/Ks* Calculator on TBtools-II, and then we determined the selection mode based on the *Ka/Ks* ratio.

Analysis of cis-acting elements in PeFAD promoter

We obtained the 1,500 bp sequences upstream of initiation codon of *PeFAD* gene from the reference genome, and then predicted the *cis*-regulatory elements on PlantCARE websites (http://bioinformatics.psb.ugent.be/webtools/plantcare/html/).

MicroRNA (miRNA) target predictions in PeFAD genes

We predicted the potential miRNAs targeting *PeFAD* genes based on all of miRNAs in database, using psRNATarget website (https://www.zhaolab.org/psRNATarget/) with the expected value of 3 and other default parameters.

Expression of *PeFAD* genes in different organs and under abiotic stresses

Expression levels of full-length *PeFAD* genes in different organs/tissues (Supplementary Table 3) as well as under abiotic stresses and phytohormone treatments including cold (NCBI accession no., GSE130314), drought, salt, SA and ABA (GSE169067), BR (GSE123529), NAA (GSE100172) and GA (GSE104596), were analyzed using published RNA-seq data, and then visualized in a heat map using TBtools-II, in which *PeFAD* genes were determined as differentially expressed genes (DEGs) if log2FC of gene expression values were ≥1 or ≤-1 and the FPKM or TPM values were also ≥1.

Expression of *PeFAD* genes in response to cold stress

The cold treatment (4 °C) of 2-months-old seedlings of moso bamboo were performed as previously described [45], the seedling leaves were sampled at 0 h, 24 h and 48 h under cold stress, and they were all immediately frozen in liquid nitrogen and stored in -80 °C. The top cold-responsive *PeSLD1* gene and its potential upstream regulatory gene *PeCBF3* were selected to perform the further qRT-PCR to validate their response to cold stress.

Chlorophyll fluorescence imaging

The fluorescence parameters (*Fv/Fm*, *NPQ* and Φ_{PSII}) and chlorophyll fluorescence images of the chia seedling leaves at 0 h, 24 h and 48 h after cold treatment were analyzed using the plant phenotype imager (device no. 20A00005; a chlorophyll fluorescence imaging system FluorCam7.0; Photon Systems Instruments, Brno, Czech Republic) as previously described [44].

RNA extraction and qRT-PCR analysis

Moso bamboo (*P. edulis*) materials were collected from the botanical garden of bamboo at Leshan Normal University (E103°68′; N29°59′). Total RNA was extracted from the moso bamboo seedling leaves under cold stress by the RNAsimple Total RNA Kit (DP419, Tiangen, Beijing) and then the first-strand total cDNA was synthesized using one μg of total RNA by the PrimeScript Reagent Kit with gDNA Eraser (Takara Dalian, China). The qRT-PCR experiment was performed using the TB Green Premix Ex Taq II (Tli RNaseH Plus) (Takara

Dalian, China) on CFX96 Real-time PCR System (Bio-Rad, USA) with 3 replicates as described on our previous report [45]. The primers for the selected *PeSLD1* and *PeCBF3* genes and the internal control gene *PeUBQ* [3] were shown in Supplementary Table 11.

Supplementary Information

The online version contains supplementary material available at https://doi.org/10.1186/s12864-024-11065-9.

Supplementary Material 1

Supplementary Material 2

Supplementary Material 3

Supplementary Material 4

Supplementary Material 5

Supplementary Material 6

Supplementary Material 7

Supplementary Material 8

Supplementary Material 9

Author contributions

Y.X. designed the study. C.F., Q.F., S.W., F.W., N.J., and R.Z. performed the experiments. C.F. and Y.X. analyzed the data. Y.X. undertook the use and maintenance of plant phenotype imager. C.F. and Y.X. wrote and revised the manuscript.

Funding

This work was supported by the Science and technology program of Leshan Normal Univerisity (2021SSDJS003), National Key Research and Development Program of China (2022YFD1901405), National Natural Science Foundation of China (32001441), Opening Foundation of Key Laboratory of Sichuan Province for Bamboo Pests Control and Resource Development (ZLKF202306), and Science and Technology Program of Leshan Normal University (2022SSDJ005, KYPY2023-0006, XJR17005, LZD010).

Data availability

The genome sequences, protein sequences and gene annotation files of *P. edulis* were downloaded in GigaDB (http://gigadb.org/dataset/view/id/100498). RNA raw data (Supplementary Table 3) for 19 different organs/tissues (GSE90517, GSE104951, GSE121216, PRJNA842835, and PRJNA217219), and abiotic stresses and hormones treatments (GSE130314, GSE169067, GSE104596, GSE100172, and GSE123529) in *P. edulis* was downloaded in NCBI database (https://www.ncbi.nlm.nih.gov/).

Declarations

Ethics approval and consent to participate

The moso bamboo (*P. edulis*) materials used in qRT-PCR analysis were taken from the botanical garden of bamboo at Key Laboratory of Sichuan Province for Bamboo Pests Control and Resource Development, Leshan Normal University, Leshan, Sichuan. The collection of plant material complied with relevant institutional, national, and international guidelines and legislation.

Consent for publication

Not applicable.

Competing interests

The authors declare no competing interests.

Received: 29 July 2024 / Accepted: 18 November 2024
Published online: 25 November 2024

References

1. Zhao H, Gao Z, Wang L, Wang J, Wang S, Fei B, Chen C, Shi C, Liu X, Zhang H, Lou Y, Chen L, Sun H, Zhou X, Wang S, Zhang C, Xu H, Li L, Yang Y, Wei Y, Yang W, Gao Q, Yang H, Zhao S, Jiang Z. Chromosome-level reference genome and alternative splicing atlas of moso bamboo (*Phyllostachys edulis*). Gigascience. 2018;7(10):giy115.
2. Liu Y, Wu C, Hu X, Gao H, Wang Y, Luo H, Cai S, Li G, Zheng Y, Lin C, Zhu Q. Transcriptome profiling reveals the crucial biological pathways involved in cold response in moso bamboo (*Phyllostachys edulis*). Tree Physiol. 2020;40(4):538–56.
3. Hu X, Liang J, Wang W, Cai C, Ye S, Wang N, Han F, Wu Y, Zhu Q. Comprehensive genome-wide analysis of the *DREB* gene family in moso bamboo (*Phyllostachys edulis*): evidence for the role of *PeDREB28* in plant abiotic stress response. Plant J. 2023;116(5):1248–70.
4. Zhang H, Zhu J, Gong Z, Zhu JK. Abiotic stress responses in plants. Nat Rev Genet. 2022;23(2):104–19.
5. He M, Qin CX, Wang X, Ding NZ. Plant unsaturated fatty acids: biosynthesis and regulation. Front Plant Sci. 2020;11:390.
6. Xiao R, Zou Y, Guo X, Li H, Lu H. Fatty acid desaturases (FADs) modulate multiple lipid metabolism pathways to improve plant resistance. Mol Biol Rep. 2022;49(10):9997–10011.
7. Hou Q, Ufer G, Bartels D. Lipid signalling in plant responses to abiotic stress. Plant Cell Environ. 2016;39(5):1029–48.
8. Lim GH, Singhal R, Kachroo A, Kachroo P. Fatty acid- and lipid-mediated signaling in plant defense. Annu Rev Phytopathol. 2017;55:505–36.
9. Liang Y, Huang Y, Liu C, Chen K, Li M. Functions and interaction of plant lipid signalling under abiotic stresses. Plant Biol (Stuttg). 2023;25(3):361–78.
10. Sun Y, Shang L, Zhu QH, Fan L, Guo L. Twenty years of plant genome sequencing: achievements and challenges. Trends Plant Sci. 2022;27(4):391–401.
11. Hajiahmadi Z, Abedi A, Wei H, Sun W, Ruan H, Zhuge Q, Movahedi A. Identification, evolution, expression, and docking studies of fatty acid desaturase genes in wheat (*Triticum aestivum* L). BMC Genomics. 2020;21(1):778.
12. Chen EZ, Yang C, Tong J, Li H, Wang T, Chen L. Genome-wide analysis of fatty acid desaturase genes in rice (*Oryza sativa* L). Sci Rep. 2019;9(1):19445.
13. Zhao X, Wei J, He L, Zhang Y, Zhao Y, Xu X, Wei Y, Ge S, Ding D, Liu M, Gao S, Xu J. Identification of fatty acid desaturases in maize and their differential responses to low and high temperature. Genes (Basel). 2019;10(6):445.
14. Zhang B, Xia P, Yu H, Li W, Chai W, Liang Z. Based on the whole genome clarified the evolution and expression process of fatty acid desaturase genes in three soybeans. Int J Biol Macromol. 2021;182:1966–80.
15. Xue Y, Chen B, Wang R, Win AN, Li J, Chai Y. Genome-wide survey and characterization of fatty acid desaturase gene family in *Brassica napus* and its parental species. Appl Biochem Biotechnol. 2018;184(2):582–98.
16. Feng J, Dong Y, Liu W, He Q, Daud MK, Chen J, Zhu S. Genome-wide identification of membrane-bound fatty acid desaturase genes in *Gossypium hirsutum* and their expressions during abiotic stress. Sci Rep. 2017;7:45711.
17. Cheng C, Liu F, Sun X, Wang B, Liu J, Ni X, Hu C, Deng G, Tong Z, Zhang Y, Lü P. Genome-wide identification of *FAD* gene family and their contributions to the temperature stresses and mutualistic and parasitic fungi colonization responses in banana. Int J Biol Macromol. 2022;204:661–76.
18. Wei H, Movahedi A, Xu S, Zhang Y, Liu G, Aghaei-Dargiri S, Ghaderi Zefrehei M, Zhu S, Yu C, Chen Y, Zhong F, Zhang J. Genome-wide characterization and expression analysis of fatty acid desaturase gene family in poplar. Int J Mol Sci. 2022;23(19):11109.
19. Niu E, Gao S, Hu W, Zhang C, Liu D, Shen G, Zhu S. Genome-wide identification and functional differentiation of fatty acid desaturase genes in *Olea europaea* L. Plants (Basel). 2022;11(11):1415.
20. Li J, Liu A, Najeeb U, Zhou W, Liu H, Yan G, Gill RA, Yun X, Bai Q, Xu L. Genome-wide investigation and expression analysis of membrane-bound fatty acid desaturase genes under different biotic and abiotic stresses in sunflower (*Helianthus annuus* L). Int J Biol Macromol. 2021;175:188–98.
21. Kidokoro S, Shinozaki K, Yamaguchi-Shinozaki K. Transcriptional regulatory network of plant cold-stress responses. Trends Plant Sci. 2022;27(9):922–35.
22. Xue Y, Wu F, Chen R, Wang X, Tseke Inkabanga A, Huang L, Qin S, Zhang M, Chai Y. Genome-wide analysis of fatty acid desaturase genes in Chia (*Salvia hispanica*) reveals their crucial roles in cold response and seed oil formation. Plant Physiol Biochem. 2023;199:107737.
23. Raboanatahiry N, Yin Y, Chen K, He J, Yu L, Li M. In silico analysis of fatty acid desaturases structures in *Camelina sativa*, and functional evaluation of *CsaFAD7* and *CsaFAD8* on seed oil formation and seed morphology. Int J Mol Sci. 2021;22(19):10857.

24. Chen M, Thelen JJ. *ACYL-LIPID DESATURASE2* is required for chilling and freezing tolerance in Arabidopsis. Plant Cell. 2013;25:1430–44.
25. Resemann HC, Herrfurth C, Feussner K, Hornung E, Ostendorf AK, Gömann J, Mittag J, van Gessel N, Vries J, Ludwig-Müller J, Markham J, Reski R, Feussner I. Convergence of sphingolipid desaturation across over 500 million years of plant evolution. Nat Plants. 2021;7(2):219–32.
26. Zhou Y, Zeng L, Fu X, Mei X, Cheng S, Liao Y, Deng R, Xu X, Jiang Y, Duan X, Baldermann S, Yang Z. The sphingolipid biosynthetic enzyme Sphingolipid delta8 desaturase is important for chilling resistance of tomato. Sci Rep. 2016;6:38742.
27. Singh AK, Raina SK, Kumar M, Aher L, Ratnaparkhe MB, Rane J, Kachroo A. Modulation of *GmFAD3* expression alters abiotic stress responses in soybean. Plant Mol Biol. 2022;110(1–2):199–218.
28. Nguyen VC, Nakamura Y, Kanehara K. Membrane lipid polyunsaturation mediated by *FATTY ACID DESATURASE 2* (*FAD2*) is involved in endoplasmic reticulum stress tolerance in *Arabidopsis thaliana*. Plant J. 2019;99(3):478–93.
29. Zhang J, Liu H, Sun J, Li B, Zhu Q, Chen S, Zhang H. Arabidopsis fatty acid desaturase FAD2 is required for salt tolerance during seed germination and early seedling growth. PLoS ONE. 2012;7(1):e30355.
30. Wang J, Shao Y, Yang X, Zhang C, Guo Y, Liu Z, Chen M. Heterogeneous expression of stearoyl-acyl carrier protein desaturase genes *SAD1* and *SAD2* from *Linum usitatissimum* enhances seed oleic acid accumulation and seedling cold and drought tolerance in *Brassica napus*. J Integr Agr. 2024;23(6):1864–78.
31. Okazaki Y, Saito K. Roles of lipids as signaling molecules and mitigators during stress response in plants. Plant J. 2014;79(4):584–96.
32. Liu H, Timko MP. Jasmonic acid signaling and molecular crosstalk with other phytohormones. Int J Mol Sci. 2021;22(6):2914.
33. Li C, Xu M, Cai X, Han Z, Si J, Chen D. Jasmonate signaling pathway modulates plant defense, growth, and their trade-offs. Int J Mol Sci. 2022;23(7):3945.
34. Lee MW, Padilla CS, Gupta C, Galla A, Pereira A, Li J, Goggin FL. The *FATTY ACID DESATURASE2* family in tomato contributes to primary metabolism and stress responses. Plant Physiol. 2020;182(2):1083–99.
35. Matsuda O, Watanabe C, Iba K. Hormonal regulation of tissue-specific ectopic expression of an Arabidopsis endoplasmic reticulum-type omega-3 fatty acid desaturase (FAD3) gene. Planta. 2001;213(6):833–40.
36. Song Z, Lai X, Chen H, Wang L, Pang X, Hao Y, Lu W, Chen W, Zhu X, Li X. Role of *MaABI5-like* in abscisic acid-induced cold tolerance of 'Fenjiao' banana fruit. Hortic Res. 2022;9:uhac130.
37. Kazaz S, Barthole G, Domergue F, Ettaki H, To A, Vasselon D, De Vos D, Belcram K, Lepiniec L, Baud S. Differential activation of partially redundant Δ9 stearoyl-ACP desaturase genes is critical for omega-9 monounsaturated fatty acid biosynthesis during seed development in Arabidopsis. Plant Cell. 2020;32(11):3613–37.
38. Li S, Castillo-González C, Yu B, Zhang X. The functions of plant small RNAs in development and in stress responses. Plant J. 2017;90(4):654–70.
39. Gai W, Sun H, Hu Y, Liu C, Zhang Y, Gai S, Yuan Y. Genome-wide identification of membrane-bound fatty acid desaturase genes in three peanut species and their expression in *Arachis hypogaea* during drought stress. Genes. 2022;13(10):1718.
40. Rizza F, Pagani D, Stanca AM, Cattivelli L. Use of chlorophyll fluorescence to evaluate the cold acclimation and freezing tolerance of winter and spring oats. Plant Breeding. 2001;120(5):389–96.
41. Mishra A, Heyer AG, Mishra KB. Chlorophyll fluorescence emission can screen cold tolerance of cold acclimated *Arabidopsis thaliana* accessions. Plant Methods. 2014;10(1):38.
42. Chen C, Wu Y, Li J, Wang X, Zeng Z, Xu J, Liu Y, Feng J, Chen H, He Y, Xia R. TBtools-II: a one for all, all for one bioinformatics platform for biological big-data mining. Mol Plant. 2023;16(11):1733–42.
43. Xue Y, Zhang C, Shan R, Li X, Tseke Inkabanga A, Li L, Jiang H, Chai Y. Genome-wide identification and expression analysis of *nsLTP* gene family in rapeseed (*Brassica napus*) reveals their critical roles in biotic and abiotic stress responses. Int J Mol Sci. 2022;23(15):8372.
44. Zhang H, Jiang C, Ren J, Dong J, Shi X, Zhao X, Wang X, Wang J, Zhong C, Zhao S, Liu X, Gao S, Yu H. An advanced lipid metabolism system revealed by transcriptomic and lipidomic analyses plays a central role in peanut cold tolerance. Front Plant Sci. 2020;11:1110.
45. Xue Y, Chen B, Win AN, Fu C, Lian J, Liu X, Wang R, Zhang X, Chai Y. Omega-3 fatty acid desaturase gene family from two ω-3 sources, *Salvia hispanica* and *Perilla frutescens*: Cloning, characterization and expression. PLoS ONE. 2018;13(1):e0191432.

Publisher's note